CONCLUSIONS

1. On the basis of operating tests with universal joints of the ZIL-130 and ZIL-133 automobiles, standard carbon steel 45 looks very promising for bulk-surface hardening of parts with working dimensions ∿30 mm.

2. After bulk-surface hardening the static and fatigue strengths of ZIL-130 universal joints of steel 45 exceed those of steel 18KhGT after carburizing.

LITERATURE CITED

1. K. Z. Shepelyakovskii, Surface Hardening of Machine Parts [in Russian], Mashinostroenie, Moscow (1972), p. 174.
2. E. I. Natanzon and L. S. Temyanko, "Simultaneous hardening of halfaxles of trucks," Avtom. Prom., No. 10 (1976).
3. V. D. Zelenova et al., "Effect of preliminary heat treatment on the dispersity of inclusions and austenite grain size," Metalloved. Term. Obrab. Met., No. 11, 30 (1966).

CHANGES IN THE STRUCTURE AND PROPERTIES OF CYLINDER SLEEVES OF INTERNAL COMBUSTION ENGINES AFTER LASER TREATMENT

V. K. Sedunov, V. M. Andriyakhin, N. T. Chekanova, and V. M. Belov

UDC 620.17:620.18:621.3.038.8:621.785:621.43

To achieve high wear resistance of the upper parts of cylinder sleeves operating with compression and oil retention rings of chromized cast iron, the upper part has an insert of high-alloy cast iron (18% Ni, 2% Cr, and 8% Cu) that is pressed into sleeves made of standard gray cast iron SCh24-44. However, this method of manufacturing cylinder sleeves is laborious and consumes large quantities of scarce alloying elements.

This work concerns an attempt to replace Niresist inserts in cylinder sleeves by hardening the gray cast iron sleeve itself by means of laser treatment. The treatment is characterized by brevity, minimal warping, lack of any need for quenchants, the possibility of treating hard-to-reach places, and limited expenditures for energy.

Samples and parts were prepared from gray cast iron with the following composition: 3.4% C, 2.40% Si, 0.55% Mn, 0.16% P, 0.55% S, 0.10% Ni. The surfaces of the samples and parts were blackened to reduce the reflecting capacity (TU 610-1532-76) before the laser treatment. The samples and parts were heated with the continuous LT-1 CO_2 gas laser. During melting the power of the laser was 3 kW and the speed of the beam 0.5 m/min, and 1 kW and 0.7 m/min, respectively, without melting; the width of the path was 5 mm. The laser

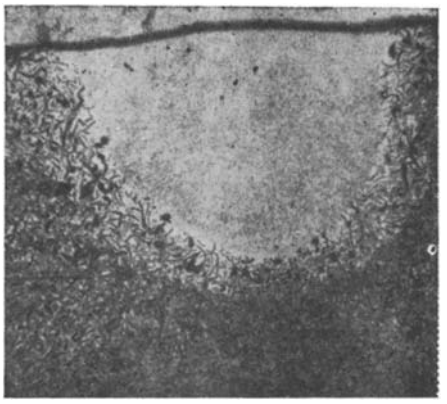

Fig. 1. Microstructure of gray cast iron SCh24-44 after laser treatment with melting. 50 ×.

Moscow Automobile Factory. Translated from Metallovedenie i Termicheskaya Obrabotka Metallov, No. 9, pp. 10-13, September, 1980.

0026-0673/80/0910-0630$07.50

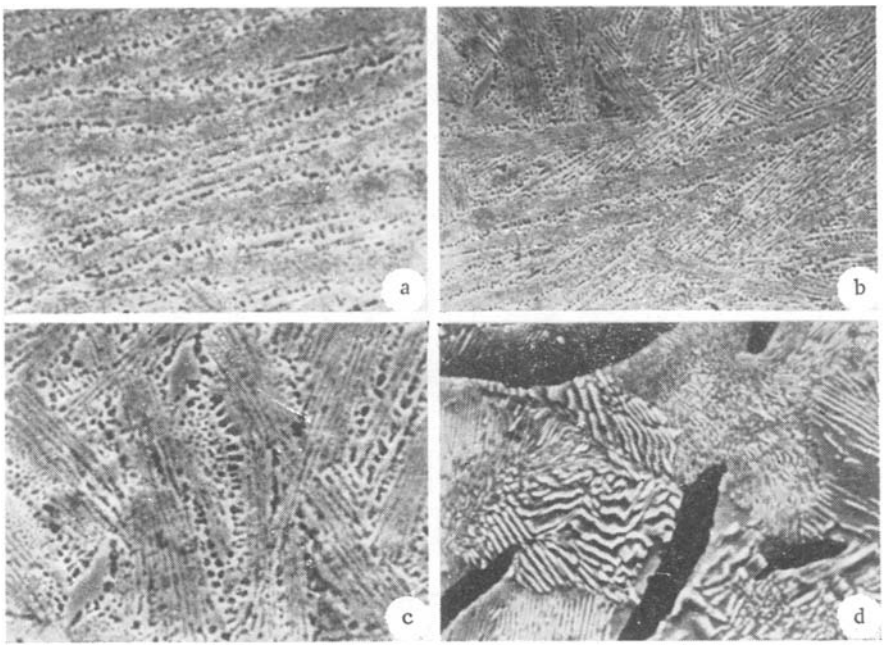

Fig. 2. Structure of pearlitic gray cast iron formed as the result of laser treatment with a high crystallization rate (2000 ×). a) Surface of melted zone; b) central section of melted zone; c) boundary of melted and unmelted zones; d) original structure.

treatment was conducted at an angle of 45° to the axis of the part along a length of 45 mm.

The structure was examined by means of light and scanning electron microscopes. Phase analysis was conducted by means of x-ray diffraction in the DRON-1 apparatus and by means of the URS-60 diffractometer, and also by Mössbauer spectroscopy.* The Mössbauer spectra were recorded with a spectrometer operating at constant acceleration with recording of the spectra by means of a multichannel LP4840 analyzer by two methods [1].

In the first method secondary γ quanta were recorded with energies of 14.4 keV and x-ray beams with an energy of 6.3 keV scattered by the sample from a surface layer 1-5 μm thick.

In the second method the sample was placed in a special counter and the Mössbauer spectra were recorded by means of conversion electrons, absorption of which by the sample was considerably greater than for x-ray beams and γ quanta, and therefore a thinner layer was analyzed — 0.1 μm. The spectra were measured in both methods by using a Mössbauer source of γ quanta ^{57}Co in a copper matrix with an activity of 30 mCi. The distribution

*The phase analysis with the DRON-1 apparatus was made by V. A. Lyakishev and the Mössbauer spectroscopy by S. I. Reiman.

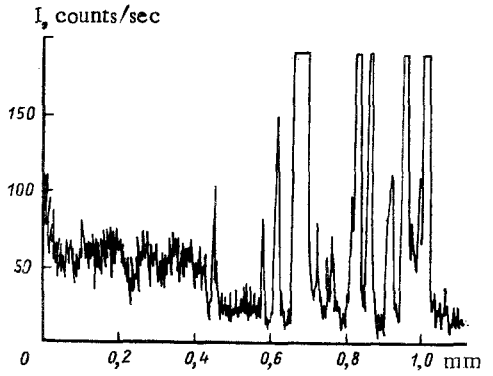

Fig. 3. Distribution of carbon in the zone of melting after laser treatment.

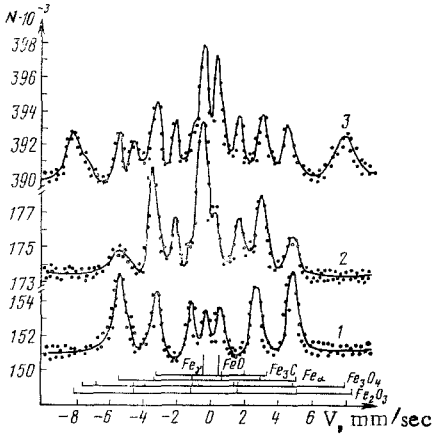

Fig. 4

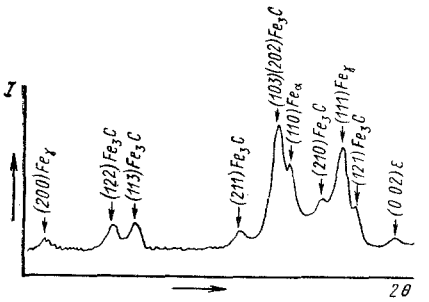

Fig. 5

Fig. 4. Mössbauer spectra of gray cast iron SCh 24-44 after laser treatment. 1) Original gray cast iron; 2) after laser treatment without melting; 3) after laser treatment with melting.

Fig. 5. Distribution of the intensity of radiation from the surface of SCh 24-44 cast iron melted with a laser.

of carbon, chromium, and manganese in the zone of laser treatment was determined by microprobe analysis with the MS-46 microanalyzer equipped with an anticontamination device for analysis of light elements. The control samples for analysis of carbon were graphite and the P-2 alloy (3.5% C, 0.32% Mo, 0.66% Cu, 0.62% N, 1.00% Mn, 0.60% Cr, 0.087% S, 0.47% P, 3.08% Si, 0.12% Al).

The microstructural analysis showed that the structures formed as the result of the laser treatment at high heating and cooling rates (10^{-3}-10^{-7} sec) and standard heat treatment differ greatly. After laser treatment there are two distinct zones (Fig. 1). In the first zone cooling occurs from the liquid condition, and with increasing etching time in 4% nital one observes a series of pits oriented at an angle of 8-15° to the surface in the form of eutectic colonies of cementite, which determine the crystallization of dendrites in this direction (Fig. 2a). With crystallization at standard cooling rates one observes a zone of columnar crystals and shrink holes that are not observed after laser treatment, and also a tendency for the volume to increase slightly. Near the central section of the zone of melting the crystallization of dendrites occurs in different directions, which is characteristic of primary cementite (Fig. 2b). At the boundary of the liquid and solid metal the dendrites are primarily perpendicular to the boundary and the size of the dendrites is several times larger than in the central section (Fig. 2c).

In the melted zone there are no graphite inclusions such as observed in gray cast iron after the standard treatment (Fig. 2d); the inclusions are completely dissolved in the liquid metal, enriching it in carbon. The high carbon content of the melted zone is confirmed by microprobe analysis (Fig. 3). The carbon concentration increases notably down to a depth of 0.05 mm, evidently due to saturation from the carbon-containing black paint. Calculations indicate that this zone contains 8-10% C. The distribution of chromium and manganese in the zone of melting and the matrix is practically the same. The hardness reaches H_{50} 1000-1200 in the melted zone and does not depend on the speed of the beam or its power. At the boundary of crystallization of the liquid metal with the unmelted metal one observes high porosity, the spheroidal shape of the pores indicating that they are formed due to evolution of gases absorbed by graphite during crystallization of the cast iron. The heat-affected zone consists of martensite, austenite, and lamellar graphite with hardness $H_{50} = 800$-1100.

Figure 4 shows ^{57}Fe Mössbauer spectra of the surface layer 1 μm thick of the original gray cast iron with a pearlitic structure (spectrum 1) and cast iron after laser treatment without melting (spectrum 2) and with melting (spectrum 3). It can be seen that the spectrum of the original gray cast iron consists mainly of a sextet, the constants of which are similar to those of spectra for α iron [2], although substantial line broadening is observed

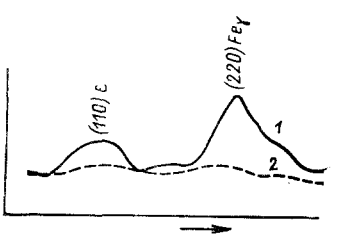

Fig. 6

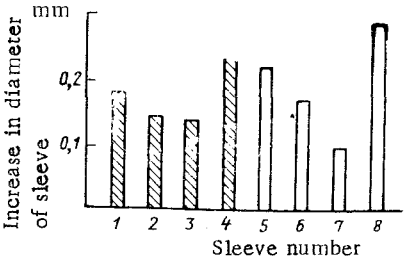

Fig. 7

Fig. 6. Distribution of the intensity of radiation from the melted surface before tempering (1) and after tempering (2) at 300° for 1.5 h.

Fig. 7. Comparative results of bench tests of experimental (hatched columns) and standard (white columns) cylinder sleeves for wear. 1-4) Laser treatment of gray cast iron SCh24-44 with melting; 5-8) standard treatment, with Niresist insert.

in this case ($\Gamma = 1.0$ mm/sec). This points to heterogeneous envelopment of iron atoms with carbon atoms, which is characteristic of the martensitic structure. Also, in the center of the spectrum there is a line ($\Gamma = 0.31$ mm/sec) whose parameters match those of γ iron. Assuming that the values of the probability of the Mössbauer effect on ^{57}Fe nuclei are similar in these phases, let us determine the concentrations of these phases from the ratio of the areas of the corresponding lines — 90 ± 3% martensite, 10 ± 3% austenite. Besides the lines corresponding to martensite and austenite, one observes lines (sextet with splitting) corresponding to cementite. Treatment of the spectra showed that the surface layer 1 μm thick contains 20 ± 5% martensite, 20 ± 5% austenite, and 60 ± 5% cementite. Layer-by-layer phase analysis showed that with increasing thickness of the layer the quantity of cementite and austenite decreases, while the amount of martensite increases. An analysis of the spectra obtained with recording of conversion electrons (Fig. 4, spectrum 3) showed that the surface layer 0.1 μm thick also has lines of FeO, Fe_3O_4, and Fe_2O_3. The total oxide concentration of this layer is 40 ± 5%, austenite 10 ± 5%, martensite 20 ± 5%, and cementite 30 ± 5%. The formation of oxides on a surface layer of this thickness is explained by the effect of oxygen from the atmosphere on the molten metal. Phase analysis also indicates that the zone of melting consists of cementite, austenite, and martensite. However, the diffraction diagrams also show several reflections that do not correspond to any of these phases (Fig. 5). Calculated data on the interplanar distances for these reflections and comparison with existing data [3, 4] indicate that the zone of melting contains metastable phases that are not observed after standard heat treatment.

Crystallization at ultrahigh cooling rates leads to formation of metastable austenite and ε phase.* The presence of phases with a high carbon content was reported in [5]. Metastable austenite does not lower the high hardness of the surface; moreover, the microhardness is H 1200 [6]. In the structure of the melted zone one observes cells with dark points resembling eutectoid graphite in a base of eutectic cementite.

After double tempering at 300° for 1.5 h the intensity of reflections of these phases decreases sharply (Fig. 6), the hardness remaining almost unchanged. The absence of metastable phases on the Mössbauer spectra is explained by the fact that we investigated massive samples in which the hardened layer was tempered in the process of the laser treatment.

After the laser treatment, tempering at 300° for 1.5 h, and final honing the cylinder sleeves were placed in a V engine that was subjected to bench tests in forced operation with abrasive wear for 50 h. The results of comparative tests of standard sleeves indicate that the wear, determined from the change in diameter in the upper dead point, is practically the same (Fig. 7). Thus, use of laser treatment for cylinder sleeves economizes high-alloy cast iron, lowers manufacturing costs, and improves the quality of production.

*Data obtained by Yu. A. Skakov.

CONCLUSIONS

1. With a high rate of crystallization from the liquid state one finds FeO, Fe_2O_3, and Fe_3O_4 (total concentration ∿40%), 10% austenite, 30% cementite, and 20% martensite in a layer 0.1 μm thick on the surface of SCh24-44 gray cast iron. At a depth of ∿1 μm the austenite and martensite comprise 20% and cementite the remainder.

2. X-ray analysis showed that in addition to cementite austenite, and martensite the cast iron also contains metastable phases, austenite, and ε phase after laser treatment, although the intensities of the reflections decrease sharply after tempering at 300°.

3. A layer as deep as 50 μm contains 8-10% C, which points to saturation of the solid solution with carbon not only with solution of graphite but also from the carbon-containing paint applied to blacken the surface before the laser treatment.

4. The hardness of the melted zone is H_{50} 1000-1200, the hardness of the heat-affected zone H_{50} 800-1100.

5. Bench tests for 50 h showed that the laser treatment of cylinder sleeves of gray cast iron SCh24-44 in V engines increases the wear resistance to the level of cylinder sleeves with Niresist inserts.

LITERATURE CITED

1. S. I. Reiman, K. P. Mitrofanov, and V. S. Shpinel', Use of Mössbauer Spectroscopy to Analyze the Phase Composition of the Surface of Massive Samples [in Russian], No. 9, Nauka, Moscow (1979), p. 170.
2. S. Hanna et al., "Spectra obtained with polarized radiation from ^{57}Fe nuclei and the hyperfine structure," in: The Mössbauer Effect [Russian translation], Yu. Kagan (ed.), IL, Moscow (1962), p. 444.
3. R. Ruhl and M. Cohen, Trans. Met. Soc. AIME, 245, 241 (1968).
4. N. V. Edneral, V. A. Lyakishev, and Yu. A. Skakov, "Structure and phase composition of Fe + 3.8% C + 4.7% Si quenched from the liquid condition," Fiz. Met. Metalloved., 43, No. 2, 426 (1977).
5. I. N. Bogachev, Metallography of Cast Iron [in Russian], Metallurgizdat, Sverdlovsk (1962), p. 17.
6. D. and K. Swoboda, Radex Rundschau, No. 3, 204 (1970).